

Cooling in reduced period optical lattices: non-zero Raman detuning

V. S. Malinovsky

MagiQ Technologies Inc., 171 Madison Avenue, Suite 1300, New York, New York 10016

P. R. Berman

*Michigan Center for Theoretical Physics, FOCUS Center,
and Physics Department, University of Michigan, Ann Arbor, MI 48109-1120*

In a previous paper [Phys. Rev. A **72**, 033415 (2005)], it was shown that sub-Doppler cooling occurs in a standing-wave Raman scheme (SWRS) that can lead to reduced period optical lattices. These calculations are extended to allow for non-zero detuning of the Raman transitions. New physical phenomena are encountered, including cooling to non-zero velocities, combinations of Sisyphus and "corkscrew" polarization cooling, and somewhat unusual origins of the friction force. The calculations are carried out in a semi-classical approximation and a dressed state picture is introduced to aid in the interpretation of the results.

PACS numbers: 32.80.Pj,32.80.Lg,32.80.-t

Keywords: sub-Doppler, cooling, Raman

I. INTRODUCTION

In a previous paper [1] (hereafter referred to as I), we have shown that sub-Doppler cooling occurs in a *standing-wave Raman scheme* (SWRS). The SWRS is particularly interesting since it is an atom-field geometry that leads to optical lattices having reduced periodicity. Reduced period optical lattices have potential applications in nanolithography and as efficient scatterers of soft x-rays. Moreover, they could be used to increase the density of Bose condensates in a Mott insulator phase when there is exactly one atom per lattice site. With the decreased separation between lattice sites, electric and/or magnetic dipole interactions are increased, allowing one to more easily carry out the entanglement needed in quantum information applications [2].

In this paper, the calculations of I, which were restricted to two-photon resonance of the Raman fields, are extended to allow for non-zero Raman detunings. There are several reasons to consider non-zero detunings. From a fundamental physics viewpoint, many new effects arise. For example, one finds that, for non-zero detuning, it is possible to cool atoms to non-zero velocities, but only if *both* pairs of Raman fields in the SWRS are present, despite the fact that the major contribution to the friction force comes from atoms that are resonant with a *single* pair of fields. This is a rather surprising result since it is the only case we know of where non-resonant atoms that act as a catalyst for the cooling. Moreover, comparable cooling to zero velocity and non-zero velocities can occur simultaneously, but the cooling mechanisms differ. We also find effects which are strangely reminiscent of normal Doppler cooling, even though conventional Doppler cooling is totally neglected in this work. A dressed atom picture is introduced to simplify the calculations in certain limits; however, *in contrast to conventional theories of laser cooling*, nonadiabatic coupling between the dressed states limits the usefulness of this approach. The non-adiabatic transitions result from the unique potentials that are encountered in the SWRS. To our knowledge, there are no analogous calculations of laser cooling in the literature.

From a practical point of view, there is also a need for calculations involving non-zero detunings. For example, in the quantum computing scheme proposed in [2], the Raman frequency differs at different sites owing to the presence of an inhomogeneous magnetic field, making it impossible to be in two-photon resonance throughout the sample. As a result, one has to assess the modifications in cooling (and eventually trapping) resulting from non-zero detunings.

The basic geometry is indicated schematically in Fig. 1. Transitions between states $|1\rangle$ and $|2\rangle$ in the Raman scheme occur through the common state $|3\rangle$ using two field modes. Consider first the effect of fields E_1 and E_2 . Field E_1 , having frequency Ω_1 and wave vector $\mathbf{k}_1 = \mathbf{k} = k\hat{\mathbf{z}}$ drives the $1 - 3$ transition while field E_2 , having frequency $\Omega_2 \approx \Omega_1 - \omega_{21}$ and wave vector $\mathbf{k}_2 \approx -\mathbf{k}$ drives the $2 - 3$ transition, where ω_{ji} is the frequency separation of levels j and i (it is assumed that $\Omega_2/c \approx \Omega_1/c$, or, equivalently, that $\omega_{21}/\omega_{31} \ll 1$). Owing to polarization selection rules or to the fact that ω_{21} is greater than the detuning $\Delta = \Omega_1 - \omega_{31}$, one can neglect any effects related to field E_1 driving the $2 - 3$ transition or field E_2 driving the $1 - 3$ transition [3]. If, in addition, the atom-field detunings on the electronic state transitions are sufficiently large to enable one to adiabatically eliminate state $|3\rangle$, one arrives at an effective two-level system in which states $|1\rangle$ and $|2\rangle$ are coupled by a two-photon "Raman field" having propagation vector $2\mathbf{k}$ and two-photon detuning $\delta = \Omega_1 - \Omega_2 - \omega_{21}$.

Imagine that we start in state $|1\rangle$. If the initial state $|1\rangle$ amplitude is spatially homogeneous, then, after a two-quantum transition, the final state (state $|2\rangle$) amplitude varies as e^{2ikz} . Such a state amplitude amplitude does

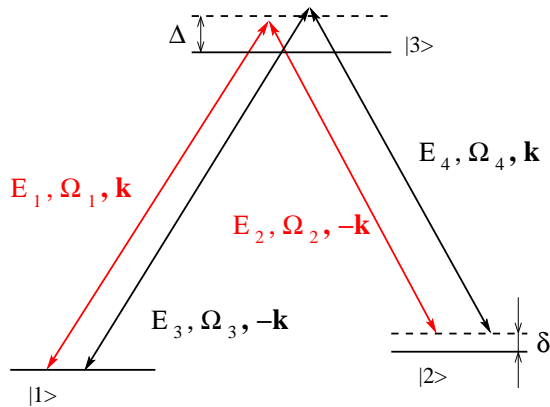


FIG. 1: Schematic representation of the energy level diagram and atom - field interaction for the standing wave Raman scheme (SWRS).

not correspond to a state $|2\rangle$ population grating, since the final state density is spatially homogeneous. To obtain a density grating one can add *another* pair of counter-propagating fields as shown in Fig. 1. These fields E_3 and E_4 differ in frequency from the initial pair, but the combined two-photon frequencies are equal,

$$\delta = \Omega_1 - \Omega_2 - \omega_{21} = \Omega_3 - \Omega_4 - \omega_{21}. \quad (1)$$

The propagation vectors are chosen such that $\mathbf{k}_3 = -\mathbf{k}_4 = -\mathbf{k}$. The frequencies of fields E_1 and E_3 are taken to be nearly equal, as are the frequencies of fields E_2 and E_4 , but it is assumed that the frequency differences are sufficient to ensure that fields E_1 and E_3 (or E_2 and E_4) do not interfere in driving *single* photon transitions, nor do fields E_1 and E_4 (or E_2 and E_3) drive Raman transitions between levels 1 and 2 [4]. On the other hand, the combined pairs of counter-propagating fields (E_1 and E_2) and (E_3 and E_4) *do* interfere in driving the 1 – 2 Raman transition and act as a “*standing wave*” Raman field which, to lowest order in the field strengths, leads to a modulation of the final state population given by $\cos(4kz)$. In this manner, a grating having period $\lambda/4$ is created.

The friction force and diffusion coefficients are calculated using a semiclassical approach. For $\delta \neq 0$, they differ qualitatively from the corresponding quantities obtained in standard Sisyphus cooling. The physical origin of the friction force was discussed in I. The calculation can also be carried out using a quantum Monte-Carlo approach, but the results of such a calculation are deferred to a future planned publication.

II. SEMI-CLASSICAL EQUATIONS

As in I, we consider the somewhat unphysical level scheme in which states $|1\rangle$ and $|2\rangle$ in Fig. 1 have angular momentum $J = 0$, while state $|3\rangle$ has angular momentum $J = 1$. The field intensities are adjusted such that the Rabi frequencies χ (assumed real) associated with all the atom-field transitions are equal (Rabi frequencies are defined by $-\mu E/2\hbar$, where μ is a component of the dipole moment matrix element between ground and excited states), and the partial decay rate of level 3 to each of levels 1 and 2 is taken equal to $\Gamma/2$ (equal branching ratios for the two transitions). The fields all are assumed to have the *same* linear polarization; there is no polarization gradient. The results would be unchanged if the fields were all σ_+ polarized.

It is assumed that the electronic state detunings are sufficiently large to satisfy

$$\Omega_1 - \omega_{31} \approx \Omega_3 - \omega_{31} \approx \Omega_2 - \omega_{32} \approx \Omega_4 - \omega_{32} \equiv \Delta \gg \Gamma, \chi. \quad (2)$$

In this limit and in the rotating-wave approximation, it is possible to adiabatically eliminate state $|3\rangle$ and to obtain equations of motion for ground state density matrix elements. With the same approximations used in I, one obtains steady-state equations, including effects related to atomic momentum diffusion resulting from stimulated emission

and absorption, and spontaneous emission. In a field interaction representation [5], the appropriate equations are [1]

$$\alpha \frac{\partial(\rho_{22} - \rho_{11})}{\partial x} = -(\rho_{22} - \rho_{11}) - 2i\sigma \cos(x) [\rho_{12} - \rho_{21}], \quad (3a)$$

$$\alpha \frac{\partial \rho_{12}}{\partial x} = -(1 + id)\rho_{12} - i\sigma \left[\cos(x) (\rho_{22} - \rho_{11}) - i\hbar k \sin(x) \frac{\partial S}{\partial p} \right] - \cos(x)S/2, \quad (3b)$$

$$\rho_{21} = \rho_{21}^*, \quad (3c)$$

or, in terms of real variables,

$$\alpha \frac{\partial}{\partial x} \begin{pmatrix} u \\ v \\ w \end{pmatrix} = \begin{pmatrix} -1 & d & 0 \\ -d & -1 & -2\sigma \cos x \\ 0 & 2\sigma \cos x & -1 \end{pmatrix} \begin{pmatrix} u \\ v \\ w \end{pmatrix} - \begin{pmatrix} \cos x S + 2\hbar k \sigma \sin x \frac{\partial S}{\partial p} \\ 0 \\ 0 \end{pmatrix}, \quad (4a)$$

where the total population S evolves as

$$\frac{\partial S}{\partial t} = \frac{7}{5}\hbar^2 k^2 \Gamma' \frac{\partial^2 S}{\partial p^2} - 4\Gamma' \sigma \hbar k \sin x \frac{\partial u}{\partial p} - \frac{3}{5}\hbar^2 k^2 \Gamma' \cos x \frac{\partial^2 u}{\partial p^2}, \quad (5)$$

and

$$u = \rho_{12} + \rho_{21}, \quad (6a)$$

$$v = i(\rho_{21} - \rho_{12}), \quad (6b)$$

$$w = \rho_{22} - \rho_{11}, \quad (6c)$$

$$S = \rho_{11} + \rho_{22}, \quad (6d)$$

with

$$x = 2kz, \quad (7a)$$

$$d = \frac{\delta}{2\Gamma'} \quad (7b)$$

$$\alpha = kv/\Gamma', \quad (7c)$$

$$\sigma = \Delta/\Gamma, \quad (7d)$$

$$\Gamma' = \Gamma \chi^2 / [\Delta^2 + (\Gamma/2)^2] \sim \chi^2 \Gamma / \Delta^2. \quad (7e)$$

Each of the functions u, v, w, S are now functions of the z -component of momentum $p = Mv$ (M is the atom's mass and v is the z -component of atomic velocity) as well as x , but it is assumed in this semiclassical approach that S is position independent. The parameter $\sigma = \Delta/\Gamma$ is assumed to be large compared with unity.

It will also prove useful to define dimensionless frequencies normalized to ω_r , momenta normalized to $\hbar k$, and energies normalized to $\hbar\omega_r$, where ω_r is the recoil frequency

$$\omega_r = \hbar k^2 / 2M, \quad (8)$$

such that $\tilde{\delta} = \delta/\omega_r$, $\tilde{\Gamma} = \Gamma/\omega_r$, $\tilde{\Gamma}' = \Gamma'/\omega_r$, $\tilde{\chi}_{eff} = \chi_{eff}/\omega_r$ ($\chi_{eff} = \chi^2 \Delta / [\Delta^2 + (\Gamma/2)^2] = \Gamma' \sigma$) is an effective two-photon Rabi frequency}, $\tilde{p} = p/\hbar k$, etc. In terms of these quantities,

$$\tilde{\chi}_{eff} = \frac{\chi^2 \Delta / \omega_r}{\Delta^2 + (\Gamma/2)^2} \equiv I, \quad (9a)$$

$$\tilde{\Gamma}' = I/\sigma, \quad (9b)$$

$$d = \tilde{\delta} \sigma / 2I, \quad (9c)$$

$$\alpha = \tilde{p} / \tilde{\Gamma}' = 2\sigma \tilde{p} / I. \quad (9d)$$

Note that I is the effective coupling strength normalized to the recoil frequency.

Equation (4a) can be written in matrix form as

$$\alpha \frac{d\mathbf{B}(x)}{dx} = -[\mathbf{A}_1 + 2\sigma \cos x \mathbf{A}_2] \mathbf{B}(x) - \mathbf{\Lambda}(x), \quad (10)$$

where

$$\mathbf{B}(x) = \begin{pmatrix} u \\ v \\ w \end{pmatrix}, \quad \mathbf{A}_1 = \begin{pmatrix} 1 & -d & 0 \\ d & 1 & 0 \\ 0 & 0 & 1 \end{pmatrix}, \quad \mathbf{A}_2 = \begin{pmatrix} 0 & 0 & 0 \\ 0 & 0 & 1 \\ 0 & -1 & 0 \end{pmatrix}, \quad (11)$$

$$\mathbf{\Lambda}(x) = \left[\cos x S(p) + 2\sigma\hbar k \sin x \frac{\partial S}{\partial p} \right] \begin{pmatrix} 1 \\ 0 \\ 0 \end{pmatrix}. \quad (12)$$

It should be noted that Eq. (10) differs *qualitatively* from the corresponding equation encountered in high intensity laser theory. Owing to the fact that decay of u, v, w is linked to spontaneous emission, the decay parameters depend on field intensity. When all frequencies are normalized to the optical pumping rate Γ' , the effective coupling strength σ is actually independent of field strength; moreover, since it is assumed that $\sigma > 1$, one is always in a "high intensity" limit. In contrast to the equations describing conventional Sisyphus cooling or high intensity laser theory, there is a source term for u , but no source term for the population difference w .

The formal solution of Eq. (10) satisfying boundary conditions resulting in a periodic solution is

$$\mathbf{B}(x) = -\frac{1}{\alpha} \int_{-\infty}^x dx' e^{-\mathbf{A}_1(x-x')/\alpha} [2\sigma \cos x' \mathbf{A}_2 \mathbf{B}(x') + \mathbf{\Lambda}(x')], \quad (13)$$

which, in terms of components, can be written as

$$u(x) = -\int_0^\infty d\tau e^{-\tau} \{2\sigma \cos(\alpha\tau - x) \sin[d\tau] w(x - \alpha\tau) + s(x - \alpha\tau) \cos[d\tau]\}, \quad (14a)$$

$$v(x) = -\int_0^\infty d\tau e^{-\tau} \{2\sigma \cos(\alpha\tau - x) \cos[d\tau] w(x - \alpha\tau) - s(x - \alpha\tau) \sin[d\tau]\}, \quad (14b)$$

$$w(x) = 2\sigma \int_0^\infty d\tau e^{-\tau} \cos(\alpha\tau - x) v(x - \alpha\tau), \quad (14c)$$

where

$$s(x) = \cos x S(p) + 2\sigma\hbar k \sin x \frac{\partial S}{\partial p}. \quad (15)$$

Substituting $v(x)$ into the equation for $w(x)$ we obtain

$$\begin{aligned} w(x) = & -4\sigma^2 \int_0^\infty d\tau e^{-\tau} \cos(\alpha\tau - x) \int_0^\infty d\tau' e^{-\tau'} \cos(\alpha(\tau + \tau') - x) \cos[d\tau'] w[x - \alpha(\tau + \tau')] \\ & + 2\sigma \int_0^\infty d\tau e^{-\tau} \cos(\alpha\tau - x) \int_0^\infty d\tau' e^{-\tau'} s[x - \alpha(\tau + \tau')] \sin[d\tau']. \end{aligned} \quad (16)$$

Once the solution for $w(x)$ is obtained, it is substituted into Eq. (14a) to determine $u(x)$ and the solution for $u(x)$ substituted into Eq. (5) for $\partial S/\partial t$. The resultant equation is averaged over a wavelength resulting in

$$\frac{\partial S}{\partial t} = \frac{7}{5} \hbar^2 k^2 \Gamma' \frac{\partial^2 S}{\partial p^2} - 4\Gamma' \sigma \hbar k \frac{\partial}{\partial p} \eta_1 - \frac{3}{5} \hbar^2 k^2 \Gamma' \frac{\partial^2}{\partial p^2} \eta_2, \quad (17)$$

where

$$\eta_1 = \overline{u(x) \sin x} = \frac{1}{2\pi} \int_0^{2\pi} dx u(x) \sin x, \quad (18a)$$

$$\eta_2 = \overline{u(x) \cos x} = \frac{1}{2\pi} \int_0^{2\pi} dx u(x) \cos x, \quad (18b)$$

and the bar indicates a spatial average ($\bar{S} = S$, by assumption). Equation (17) is then compared with the FokkerPlanck equation

$$\frac{\partial S}{\partial t} = \frac{\partial}{\partial p} \left[-\bar{F} S + \bar{D}_{st} \frac{\partial S}{\partial p} + \frac{\partial}{\partial p} [\bar{D}_{sp} S] \right], \quad (19)$$

to extract the spatially averaged friction \bar{F} , stimulated diffusion \bar{D}_{st} , and spontaneous diffusion \bar{D}_{sp} coefficients.

III. SOLUTIONS

A. Backward recursion method

Equation (16) can be solved using Fourier series and a backwards recursion scheme [6, 7], as outlined in the Appendix. In this manner one obtains

$$\bar{F} = -2\hbar k \sigma \Gamma' \xi_f, \quad (20a)$$

$$\bar{D}_{st} = 4\hbar^2 k^2 \sigma^2 \Gamma' \xi_{st}, \quad (20b)$$

$$\bar{D}_{sp} = \hbar^2 k^2 \Gamma' \left(\frac{7}{5} + \frac{3}{10} \xi_{sp} \right), \quad (20c)$$

where ξ_f , ξ_{sp} , ξ_{st} are given as Eq. (A17) in the Appendix. An analytic solution for the ξ s can be found only for $d = 0$ [$\xi_f(d = 0) = \alpha(1 + \alpha^2)^{-1}$, $\xi_{sp}(0) = \xi_{st}(0) = (1 + \alpha^2)^{-1}$]; otherwise, these quantities must be obtained via the recursive solutions. The effective field strength parameter in this problem is σ and one might expect that σ/α recursions are needed to solve Eqs. (A6) accurately [6, 7]. Actually, the number of recursions required depends in a somewhat complicated manner on the values of several parameters. Each recursion introduces resonances at specific values of α which can be interpreted as Stark-shifted, velocity tuned resonances [8]. For example, with $d = 0$, the lowest order recursive solution has a very strong (proportional to σ^2), narrow resonance at $\alpha^2 = 3/5$, but the second order approximation removes the divergence, while introducing yet a second resonance. Some of these velocity tuned resonances are seen in some of the graphs presented below. For $d > 1$, an upper bound for the number of recursions required to map out all the resonances is of order $(\sigma/d)(\sigma/\alpha)$; for $d \ll 1$ or $d/\sigma \gg 1$ only a few terms are needed. Even if only a single recursion is needed, the general expressions for ξ_f , ξ_{sp} , ξ_{st} are still fairly complicated.

For $d \ll 1$ one finds corrections of order d^2 to the analytical results, but owing to their complexity, these expressions are not given here. For $d/\sigma \gg 1$, one finds that, near $\alpha = 0$

$$\xi_f \sim \frac{2\alpha}{1 + 4\alpha^2} \left(\frac{\sigma}{d} \right)^2, \quad (21a)$$

$$\xi_{st} \sim \frac{1}{1 + 4\alpha^2} \left(\frac{\sigma}{d} \right)^2, \quad (21b)$$

$$\xi_{sp} \sim \frac{(3 + 8\alpha^2)}{1 + 4\alpha^2} \left(\frac{\sigma}{d} \right)^2, \quad (21c)$$

and near $\alpha = \pm d$

$$\xi_f \sim \frac{f_{\pm}}{2(1 + f_{\pm}^2 + \sigma^2)}, \quad (22a)$$

$$\xi_{st} \sim \frac{1}{2(1 + f_{\pm}^2 + \sigma^2)}, \quad (22b)$$

$$\xi_{sp} \sim \frac{1 + \sigma^2}{2(1 + f_{\pm}^2 + \sigma^2)}, \quad (22c)$$

where $f_{\pm} = (\alpha \mp d)$.

In the limit $d \gg \sigma > 1$, the friction force as a function of α contains three dispersion-like structures centered at $\alpha = 0, \pm d$. This implies that atoms can be cooled to these values of α . The amplitude of the component centered at $\alpha = 0$ is of order σ^2/d^2 while its width is of order unity. On the other hand, the amplitude of the components centered at $\alpha = \pm d$ are of order $1/\sigma$ while their width are of order σ . It is shown below that the central peak in the momentum distribution is negligible compared with the two side peaks in the limit $d \gg \sigma > 1$; that is, in this limit cooling occurs more efficiently to velocities $\alpha = \pm d$ for which the atoms are Doppler shifted into resonance with the two-photon transitions connecting levels 1 and 2. The width of the $\alpha = \pm d$ components is similar to that found in sub-Doppler cooling in magnetic fields (MILC) [9]; in both MILC and the SWRS, the qualitative dependence for the friction coefficient as a function of α is similar to that found in sub-Doppler cooling using "corkscrew" polarization [10]. As such, the curve is "power broadened," since the effective field strength in the problem is σ .

It is tempting to consider the contribution to the friction force near $\alpha = d$ as arising from the *single* pair of fields (E_1 and E_2), since these fields are nearly resonant with the 1-2 transition in a reference frame moving at $2kv = \delta$. Tempting as it may be, this interpretation is wrong, since we have already shown in I that, for a single pair of Raman fields, the friction force vanishes *identically*, regardless of detuning. Thus, it is necessary that the second pair of fields

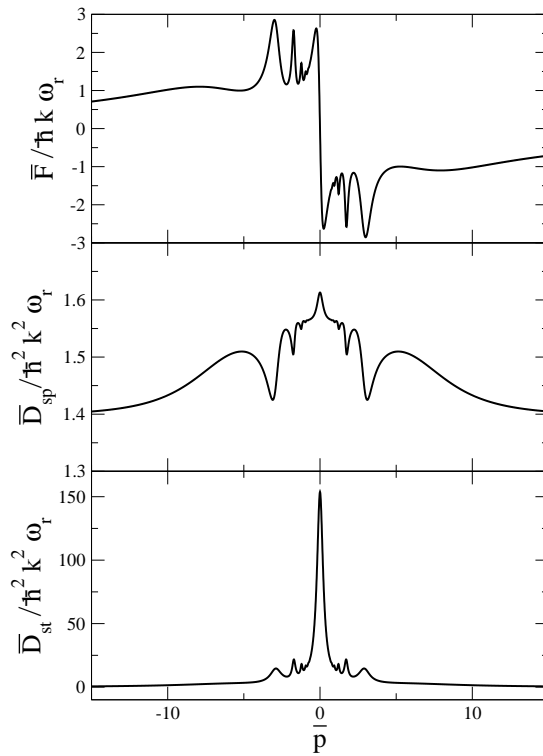


FIG. 2: Averaged force and diffusion coefficients in dimensionless units as a function of scaled momentum $\bar{p} = p/\hbar k$ for $I = 10$, $\sigma = 10$, and $\tilde{\delta} = 20$.

be present, even if they are far off resonance with atoms satisfying $2kv = \delta$. The main effect of the second pair of fields is to cancel the contribution to the force from the population difference between levels 1 and 2 (see Appendix A in I), leaving the contribution from the 1-2 coherence only ($u = \rho_{12} + \rho_{21}$). Near $2kv = \delta$ the major contribution to u does come from atoms that are nearly resonant with the 1-2 transition in a reference frame moving at $2kv = \delta$, but the scattering of the second pair of fields (E_3 and E_4) from the population difference created by the resonant pair of fields modifies the net force on the atoms. In some sense, one can view the second pair of fields as enabling the cooling at $2kv = \delta$. Note that the magnitude of the damping coefficient is down by σ^2 from that at $d = 0$; it is of the same order as that found in sub-Doppler cooling using "corkscrew" polarization [10].

For arbitrary values of α and δ , with σ of order 10, the recursive solution converges very rapidly for most values of α and numerical solutions can be obtained quickly and easily. Two examples are shown in Figs. 2 and 3, where the averaged friction force \bar{F} in units of $\hbar k \omega_r$ and the averaged diffusion coefficients \bar{D}_{st} and \bar{D}_{sp} in units $\hbar^2 k^2 \omega_r$ are plotted as a function of the scaled momentum $\bar{p} = p/\hbar k$. In terms of the ξ s defined by Eqs (20), these quantities can be written as

$$\begin{aligned}\bar{F}/\hbar k \omega_r &= -2I \xi_f(\alpha = 2\sigma \bar{p}/I), \\ \bar{D}_{st}/\hbar^2 k^2 \omega_r &= 4\sigma I \xi_{st}(\alpha = 2\sigma \bar{p}/I), \\ \bar{D}_{sp}/\hbar^2 k^2 \omega_r &= I \left[\frac{7}{5} + \frac{3}{10} \xi_{sp}(\alpha = 2\sigma \bar{p}/I) \right] / \sigma.\end{aligned}$$

In Fig. 2, $I = 10$, $\sigma = 10$, and $\tilde{\delta} = \delta/\omega_r = 20$. One sees in these curves a number of velocity tuned resonances under a "power-broadened" envelope [8]. In Fig. 3, $I = 10$, $\sigma = 10$, and $\tilde{\delta} = 220$, implying that $d = 110$ and $\sigma/d = 1/11$. In this limit Eqs. (21), (22) are valid and we see three contributions to the averaged force and diffusion coefficients. The values of the force and diffusion coefficients near the Doppler tuned resonances at $\bar{p} = \pm \tilde{\delta}/4$ are typical of corkscrew polarization cooling [10], and the ratio of the force to diffusion coefficient is of order $1/\hbar k$. On the other hand, this ratio is of order $1/\hbar k \sigma$ near $\bar{p} = 0$, a result that is typical of Sisyphus cooling in a lin⊥lin geometry; however, both the friction and diffusion coefficients are smaller than those in conventional Sisyphus cooling by a factor $(\sigma/d)^2$ when $\sigma/d \ll 1$. As a consequence, the cooling is dominated by the contributions near $\bar{p} = \pm \tilde{\delta}/4$ when $\sigma/d \ll 1$.

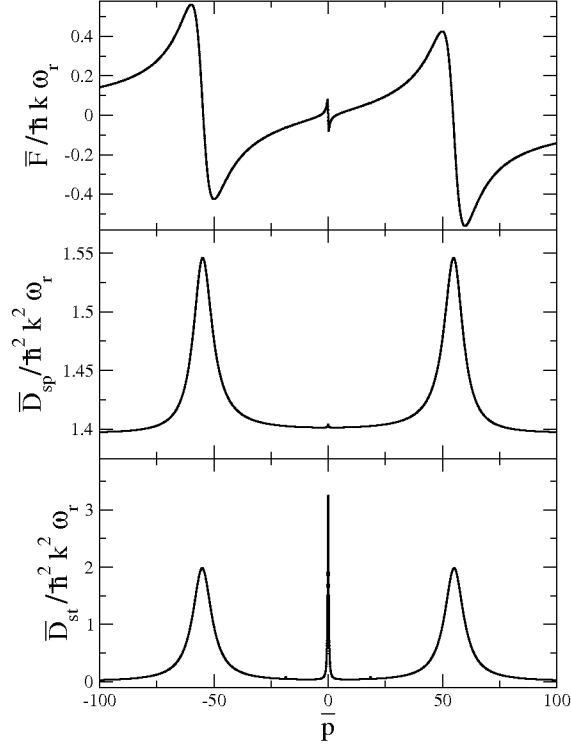


FIG. 3: Same as Fig. 2, with $I = 10$, $\sigma = 10$, and $\tilde{\delta} = 220$.

B. Iterative Solution

Since the effective field strength is always greater than unity, perturbative solutions of Eqs (10) are not of much use. However, one can get a very rough qualitative estimate of the dependence on detuning of the friction and diffusion coefficients near $\alpha = 0$ by considering an iterative solution of Eqs. (10) in powers of α . This will work only in the limit that $\alpha < 1$, so it cannot correctly reproduce the contributions to the friction and diffusion coefficients at $\alpha = \pm d$ when $d \gg \sigma > 1$. The iterative solution is useful mainly when $d^2 \lesssim \sigma^2$, since, in this limit, the dominant contribution to the momentum distribution comes from the region near $\alpha = 0$.

The iterative solution is straightforward, but algebraically ugly. To order α , one obtains from Eqs. (10)

$$\mathbf{B}(x) = -\mathbf{A}^{-1}(x) \left\{ [\mathbf{\Lambda}(x)] - \alpha \frac{d}{dx} (\mathbf{A}^{-1}(x) [\mathbf{\Lambda}(x)]) \right\}, \quad (23)$$

where $\mathbf{A}(x) = [\mathbf{A}_1 + 2\sigma \cos x \mathbf{A}_2]$. When the u component of $\mathbf{B}(x)$ is extracted from this solution and the result is substituted into Eqs. (18), all the integrals can be carried out analytically and one finds

$$\begin{aligned} \eta_1 &= -2\xi_1^{(0)} g - 2\alpha \xi_1^{(1)} S, \\ \eta_2 &= -2\xi_2^{(0)} S + 2\alpha \xi_2^{(1)} g, \end{aligned}$$

where

$$g = 2\sigma\hbar k \frac{\partial S}{\partial p}, \quad (24a)$$

$$\xi_1^{(0)} = 1 - \frac{2d^2}{\gamma_d(\gamma_d + \gamma_\sigma)}, \quad (24b)$$

$$\xi_2^{(0)} = 1 - \frac{2d^2}{\gamma_\sigma(\gamma_d + \gamma_\sigma)}, \quad (24c)$$

$$\xi_1^{(1)} = \xi_2^{(1)} = 1 - \frac{d^2 [\gamma_\sigma^2 \gamma_d^2 + \gamma_d^2 + \gamma_\sigma^2]}{\gamma_\sigma^3 \gamma_d^3}, \quad (24d)$$

$$\gamma_d = \sqrt{1 + d^2}, \quad \gamma_\sigma = \sqrt{1 + d^2 + 4\sigma^2}. \quad (24e)$$

By comparing Eqs. (17), (19) and neglecting the contribution from the second term in the equation for η_2 (since it is of relative order $\hbar k/p$), we extract the spatially averaged friction and diffusion coefficients

$$\bar{F} = -2\hbar k \sigma \Gamma' \alpha \xi_1^{(1)}, \quad (25a)$$

$$\bar{D}_{st} = 4\hbar^2 k^2 \sigma^2 \Gamma' \xi_1^{(0)}, \quad (25b)$$

$$\bar{D}_{sp} = \hbar^2 k^2 \Gamma' \left(\frac{7}{5} + \frac{3}{10} \xi_2^{(0)} \right). \quad (25c)$$

These are all even functions of the detuning d .

The spatially averaged form factors $\xi_1^{(0)}, \xi_2^{(0)}, \xi_1^{(1)}$ are equal to unity for $d = 0$, but vary as

$$\xi_2^{(0)} \approx \xi_1^{(0)} \approx (3/2)\xi_1^{(1)} \sim 3\sigma^2/d^2 \quad (26)$$

for $d \gg d/\sigma \gg 1$, in agreement with Eqs. (21). In this limit, both \bar{F} and \bar{D}_{ind} approach zero, but \bar{D}_{sp} approaches a finite value since Rayleigh scattering of the fields is independent of δ for $\delta \ll \Delta$. The friction force when $d \gg d/\sigma \gg 1$ is given by

$$\bar{F} \sim -4\Gamma' \hbar k \sigma \alpha \sigma^2 / d^2 = -16\hbar k^2 v [\Gamma(\Delta\delta/\Gamma^2)] (\chi^2/\Delta)^2 / \delta^3.$$

This equation is strangely reminiscent of the equation for Doppler cooling of two-level atoms by an off-resonant standing wave field where one finds

$$\bar{F}_{DC} \approx -4\hbar k (kv) \Gamma(\chi^2) / \Delta^3,$$

taking into account the fact that twice the momentum is transferred in a two-photon process. For the expressions to agree, one must associate a "two-photon spontaneous scattering rate" $\Gamma_{tp} = \Gamma(\Delta\delta/\Gamma^2)$ with the Raman transitions.

Of course, if $d/\sigma \gg 1$, the contributions to the friction and diffusion coefficients near $\alpha = \pm d$ become dominant insofar as they affect the momentum distribution. In this limit one cannot use the iterative solution to estimate the equilibrium temperature since the contributions from higher velocity components play a significant role.

C. Dressed State Solution

The effective Hamiltonian for the SWRS, neglecting decay is

$$H = \frac{\hbar}{2} \begin{pmatrix} \delta & 4\chi_{eff} \cos x \\ 4\chi_{eff} \cos x & -\delta \end{pmatrix}. \quad (27)$$

By diagonalizing this Hamiltonian one obtains semiclassical dressed states whose energies, as a function of x are said to characterize the optical potentials associated with this problem. It turns out that the use of dressed states in the SWRS is of somewhat limited use, owing to *nonadiabatic* coupling between the potentials. Nevertheless, the dressed states do provide additional insight to the cooling dynamics.

The eigenvalues of H are given by

$$\lambda_{\pm} = \pm \hbar R / 2, \quad R = \sqrt{\delta^2 + R_0^2}, \quad (28)$$

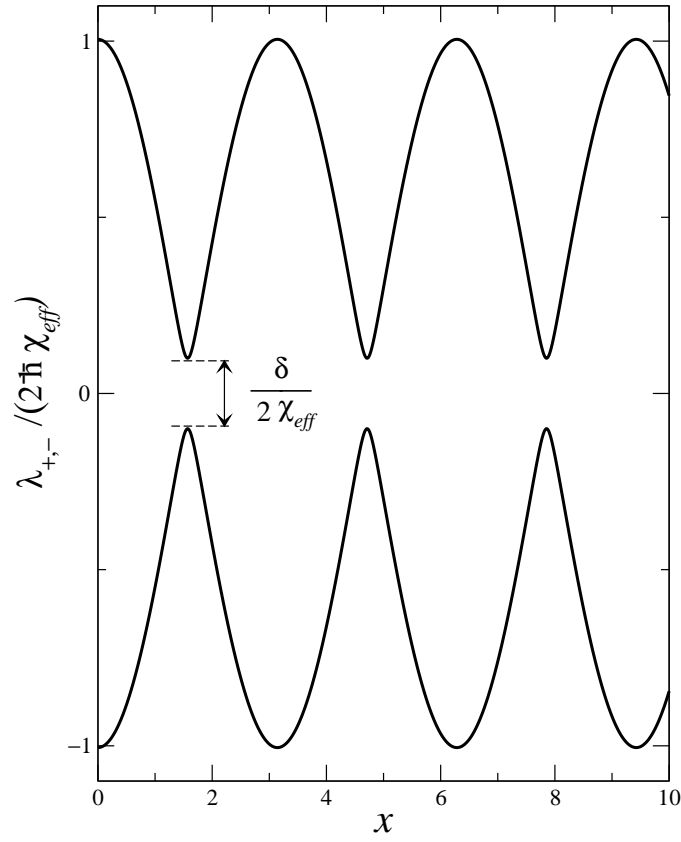


FIG. 4: Dressed state potentials.

along with eigenkets

$$|A\rangle = c|1\rangle + s|2\rangle, \quad (29a)$$

$$|B\rangle = -s|1\rangle + c|2\rangle, \quad (29b)$$

where

$$c = \cos \theta, \quad s = \sin \theta, \quad (30a)$$

$$R_0 = 4\chi_{eff} \cos x, \quad (30b)$$

$$\cos(2\theta) = \delta/R, \quad \sin(2\theta) = R_0/R, \quad 0 \leq \theta \leq \pi/2. \quad (30c)$$

The optical potentials are sketched in Fig. 4. As $\delta/2\chi_{eff}$ tends towards zero, the potentials "touch" whenever $\cos x = 0$. As is seen below, nonadiabatic transitions occur at such points [11].

Defining dressed state amplitudes via

$$\mathbf{a}_D = \mathbf{T}\mathbf{a} \quad (31)$$

with

$$\mathbf{a}_D = \begin{pmatrix} a_A \\ a_B \end{pmatrix}; \quad \mathbf{a} = \begin{pmatrix} a_1 \\ a_2 \end{pmatrix}; \quad \mathbf{T} = \begin{pmatrix} c & s \\ -s & c \end{pmatrix}$$

and a dressed state density matrix $\rho_D = \mathbf{a}_D \mathbf{a}_D^\dagger$, one can transform Eqs. (4), (6) into the dressed basis as

$$\alpha \frac{\partial w_D}{\partial x} = -w_D + \sin(2\theta) \left[\cos(x)S + 2\sigma\hbar k \sin(x) \frac{\partial S}{\partial p} \right] - \frac{\sin(2\theta)v_D}{2\sigma} + 2\alpha \frac{\partial \theta}{\partial x} (\rho_{AB} + \rho_{BA}), \quad (32a)$$

$$\alpha \frac{\partial \rho_{AB}}{\partial x} = -(1+iD)\rho_{AB} - \cos(2\theta) \left[\frac{1}{2} \cos(x)S + \sigma\hbar k \sin(x) \frac{\partial S}{\partial p} \right] - \frac{i \sin(2\theta)w_D}{2\sigma} + \alpha \frac{\partial \theta}{\partial x} (\rho_{BB} - \rho_{BA}), \quad (32b)$$

$$\frac{\partial S}{\partial t} = \frac{7}{5} \hbar^2 k^2 \Gamma' \frac{\partial^2 S}{\partial p^2} - 4\Gamma' \sigma \hbar k \sin x \frac{\partial [\cos(2\theta)u_D - \sin(2\theta)w_D]}{\partial p} - \frac{3}{5} \hbar^2 k^2 \Gamma' \cos x \frac{\partial^2 [\cos(2\theta)u_D - \sin(2\theta)w_D]}{\partial p^2}, \quad (32c)$$

$$u_D = \rho_{AB} + \rho_{BA}, \quad v_D = i(\rho_{BA} - \rho_{AB}), \quad w_D = \rho_{BB} - \rho_{AA}, \quad (32d)$$

$$\rho_{BA} = \rho_{AB}^*, \quad (32e)$$

$$D = R/2\Gamma'. \quad (32f)$$

For $\sigma \gg 1$, the terms varying as σ^{-1} can be dropped. If one also neglects the nonadiabatic coupling proportional to $\partial\theta/\partial x$, Eqs. (32) have the *remarkable* property that, even in the presence of dissipation, the equations for the dressed state coherences and populations are completely decoupled. Assuming for the moment that such an approximation is valid, one has the immediate solution

$$\rho_{AB} = -(\alpha)^{-1} \int_{-\infty}^x dx' \cos[2\theta(x')] \left[\frac{1}{2} \cos(x')S + \sigma\hbar k \sin(x') \frac{\partial S}{\partial p} \right] \exp[-(1+iD)(x-x')/\alpha]; \quad (33a)$$

$$w_{AB} = (\alpha)^{-1} \int_{-\infty}^x dx' \sin[2\theta(x')] \left[\cos(x')S + 2\sigma\hbar k \sin(x') \frac{\partial S}{\partial p} \right] \exp[-(x-x')/\alpha]. \quad (33b)$$

It then follows from Eqs. (32), and (19) that the spatially averaged friction and diffusion coefficients are given by

$$\bar{F} = 4\hbar k \sigma \Gamma' \overline{\sin(x) \{ \cos[2\theta(x)] [C(x) + C^*(x)] - \sin[2\theta(x)] A(x) \}}, \quad (34a)$$

$$\bar{D}_{st} = -8\hbar^2 k^2 \sigma^2 \Gamma' \overline{\sin(x) \{ \cos[2\theta(x)] [D(x) + D^*(x)] - \sin[2\theta(x)] B(x) \}}, \quad (34b)$$

$$\bar{D}_{sp} = \hbar^2 k^2 \Gamma' \left(\frac{7}{5} + \frac{3}{10} \overline{\cos(x) \{ \cos[2\theta(x)] [C(x) + C^*(x)] - \sin[2\theta(x)] A(x) \}} \right), \quad (34c)$$

where

$$A(x) = (\alpha)^{-1} \int_{-\infty}^x dx' \sin[2\theta(x')] \cos(x') \exp[-(x-x')/\alpha],$$

$$B(x) = (\alpha)^{-1} \int_{-\infty}^x dx' \sin[2\theta(x')] \sin(x') \exp[-(x-x')/\alpha],$$

$$C(x) = -(2\alpha)^{-1} \int_{-\infty}^x dx' \cos[2\theta(x')] \cos(x') \exp[-(1+iD)(x-x')/\alpha],$$

$$D(x) = -(2\alpha)^{-1} \int_{-\infty}^x dx' \cos[2\theta(x')] \sin(x') \exp[-(1+iD)(x-x')/\alpha],$$

and the bar indicates a spatial average. In general, the integrals and spatial averages must be calculated numerically.

In contrast to other dressed state theories, the dressed states here are of limited use since the nonadiabatic coupling is always significant. This is related to the fact that the decay constants are intimately related to the coupling strength, that the potentials periodically approach one another, and that the nonadiabatic coupling is maximal at these close separations [$\partial\theta/\partial x \sim (\sigma/d) \sin x$]. The dressed picture gives a reasonable approximation to the friction and diffusion coefficients when $|\alpha \pm d| \gg 1$ and $d \gtrsim \sigma \gg 1$. In this limit one can make a secular approximation and ignore the contribution from the $C(x)$ and $D(x)$ terms in Eqs. (34). The nonadiabatic terms neglected in Eq. (32) are of order $\sigma\alpha/d^2$ in this limit. Thus, the approximation is valid for relatively large detunings and values of α less than or on

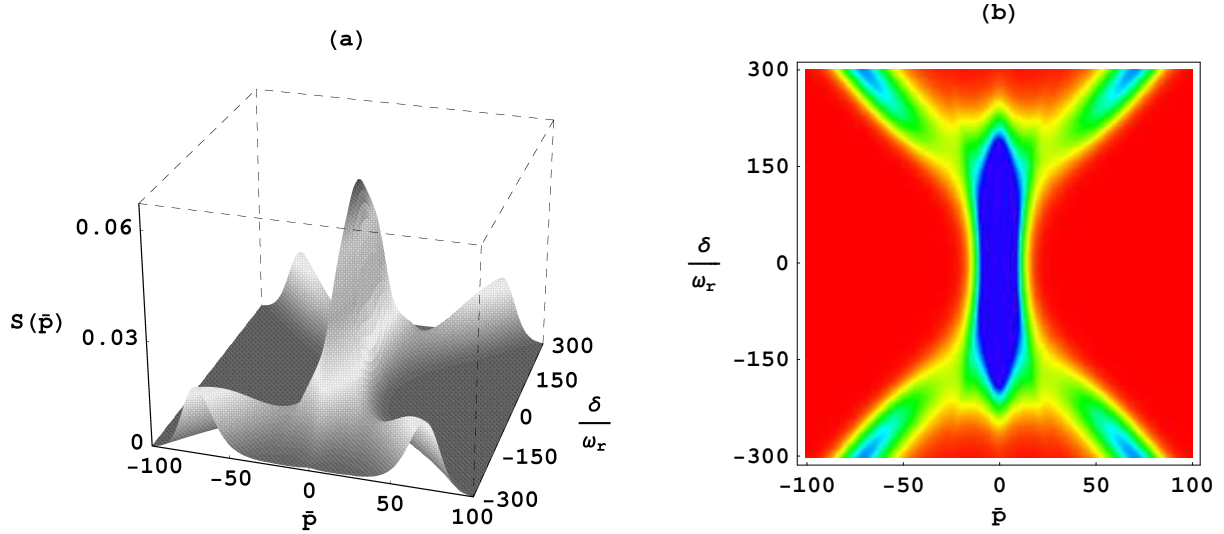


FIG. 5: The momentum distribution $S(\bar{p})$ as a function of $\bar{\delta} = \delta/\omega_r$ for $I = 40$, $\sigma = 10$; 3-dimensional plot (a) and density plot (b).

the order of unity. Indeed, in the limit $\sigma/d \ll 1$, the dressed picture results reproduce those of Eq. (21) provided α is not too large. On the other hand, they do not reproduce those of Eq. (22) near the Doppler shifted two-photon resonances; the dressed results vary as $(1 + f^2)^{-1}$ rather than $(1 + f^2 + \sigma^2)^{-1}$. Both the secular approximation and the neglect of nonadiabatic coupling break down near these two-photon resonances.

For the nonadiabatic coupling to be negligible compared with convective derivatives such as $\alpha \partial w_D / \partial x$, it is necessary that $\partial \theta / \partial x \ll 1$. It can be shown that in the regions of closest approach of the potentials that $\partial \theta / \partial x \sim \chi_{eff} / \delta = \sigma / d$. Thus, for the dressed picture to be valid, one is necessarily in the region where the approximate solutions Eqs.(21), (22) are all that is needed.

D. Density matrix solution

As a final approximate approach one can adiabatically eliminate ρ_{12} and ρ_{21} from Eqs.(3). This procedure will allow one to obtain an analytical solution for all density matrix elements in terms of a sum over Bessel functions. Such an approach is valid for $\delta \gg \Gamma'$ and $\delta \gg \chi^2 / \Delta$ so it has a limited range of applicability. The detailed results are not presented here.

IV. MOMENTUM AND ENERGY DISTRIBUTIONS

In terms of the normalized momentum $\bar{p} = p/\hbar k$, the steady state solution of the Fokker-Planck equation,

$$\frac{\bar{D}_{tot}}{\hbar k} \frac{\partial S}{\partial \bar{p}} = \left(\bar{F} - \frac{1}{\hbar k} \frac{\partial \bar{D}_{sp}}{\partial \bar{p}} \right) S, \quad (35)$$

subject to the boundary condition $\partial S / \partial p|_{p=0} = 0$, is

$$S(\bar{p}) = S_0 \exp \left\{ \hbar k \int_0^{\bar{p}} d\bar{p}' \frac{\left(\bar{F} - \frac{1}{\hbar k} \frac{\partial \bar{D}_{sp}}{\partial \bar{p}'} \right)}{\bar{D}_{tot}} \right\}, \quad (36)$$

where

$$S_0 = \left[\int_{-\infty}^{\infty} d\bar{p} \exp \left\{ \hbar k \int_0^{\bar{p}} d\bar{p}' \frac{\left(\bar{F} - \frac{1}{\hbar k} \frac{\partial \bar{D}_{sp}}{\partial \bar{p}'} \right)}{\bar{D}_{tot}} \right\} \right]^{-1}. \quad (37)$$

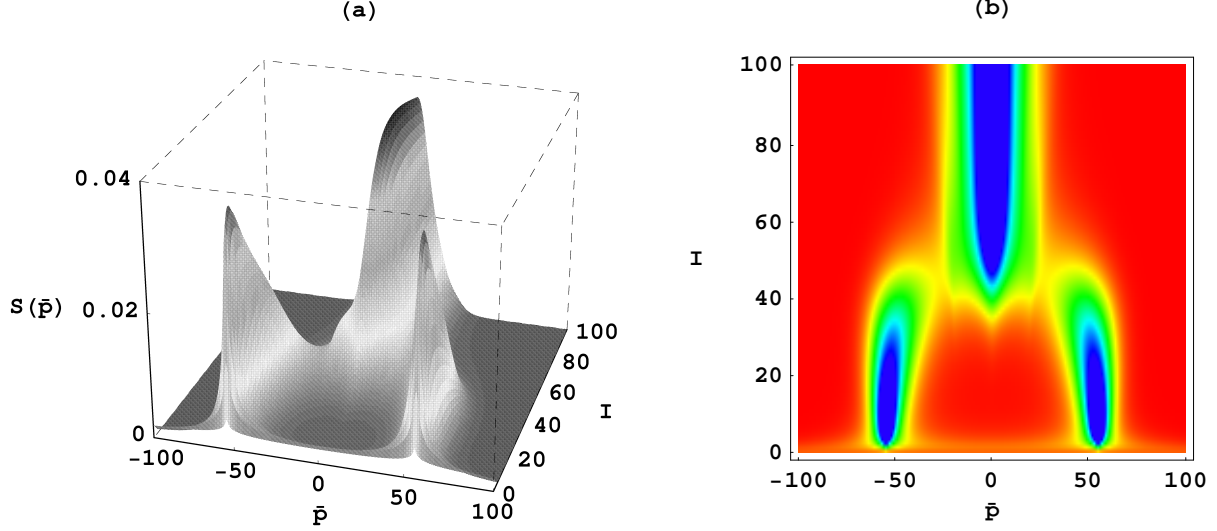


FIG. 6: The momentum distribution $S(\bar{p})$ as a function of I for $\tilde{\delta} = 220$, $\sigma = 10$; 3-dimensional plot (a) and density plot (b).

Taking into account definitions, Eq.(20), we obtain

$$S(\bar{p}) = S_0 \exp \left\{ - \int_0^{\bar{p}} d\bar{p}' \frac{2\sigma\xi_f}{\frac{7}{5} + \frac{3}{10}\xi_{sp} + 4\sigma^2\xi_{st}} \right\}, \quad (38)$$

where the ξ s are define in Eqs.(A17) and we neglect the term $(1/\hbar k) \partial \bar{D}_{sp} / \partial \bar{p}'$.

The momentum distribution $S(\bar{p})$ is plotted in Fig. 5 as a function of $\tilde{\delta}$ for $\sigma = 10$ and $I = 40$ and in Fig. 6 as a function of I for $\sigma = 10$ and $\tilde{\delta} = 220$. The curves in Fig. 7 are cuts of Fig. 5 for $\tilde{\delta} = 0, 170, 220$, and 300. When $d/\sigma = \tilde{\delta}/2I \ll 1$ and $I \gg \sigma > 1$, there is a central component having width of order $\sqrt{2I} \left(1 + \tilde{\delta}^2/8I^2\right)^{1/2}$, that is estimated using Eqs. (24). For $d/\sigma = \tilde{\delta}/2I \gg 1$, the momentum distribution breaks into three components centered at $\bar{p} = 0, \pm\tilde{\delta}/4$ [$2kv = 0, \pm\delta$], with the central component negligibly small compared with the side peaks {relative strength of side to central peak scales roughly as $(d/\sigma)^{5I/14}$, estimated using Eqs. (21), (22)}. The width of the side peaks for $d/\sigma = \tilde{\delta}/2I \gg 1$ also scale as \sqrt{I} , although they are slightly broader than the central peak when $d/\sigma = \tilde{\delta}/2I \ll 1$, reflecting the fact that the side peak cooling is of the corkscrew polarization nature, while the central component cooling for $d/\sigma \ll 1$ is of the Sisyphus nature. For intermediate values of d/σ three peaks in the momentum distribution are seen clearly; for example, when $\tilde{\delta} = 220$, $I = 40$, $\sigma = 10$, the amplitudes of the three peaks are equal.

The mean equilibrium kinetic energy can be calculated according to

$$\tilde{E} = E_{eq}/E_r = \int_{-\infty}^{\infty} d\bar{p} \bar{p}^2 S(\bar{p}), \quad (39)$$

where $E_r = \hbar\omega_r$ is the recoil energy. This quantity must be calculated numerically, in general. However, for $d/\sigma = \tilde{\delta}/2I \ll 1$ and $I \gg \sigma > 1$, one can estimate that $\tilde{E} = I \left(1 + \tilde{\delta}^2/8I\right)^{1/2}$, using Eqs.(24). For $d/\sigma = \tilde{\delta}/2I \gg 1$, the side peaks lead to an equilibrium energy that scales as $(\tilde{\delta}/4)^2$ since momentum components at both $\bar{p} = \pm\tilde{\delta}/4$ are present; however, the energy width associated with each side peak scales as I . In Fig.8, we plot $\tilde{E} = E_{eq}/E_r$ as a function of I for $\sigma = 10$ and several values of $\tilde{\delta}$.

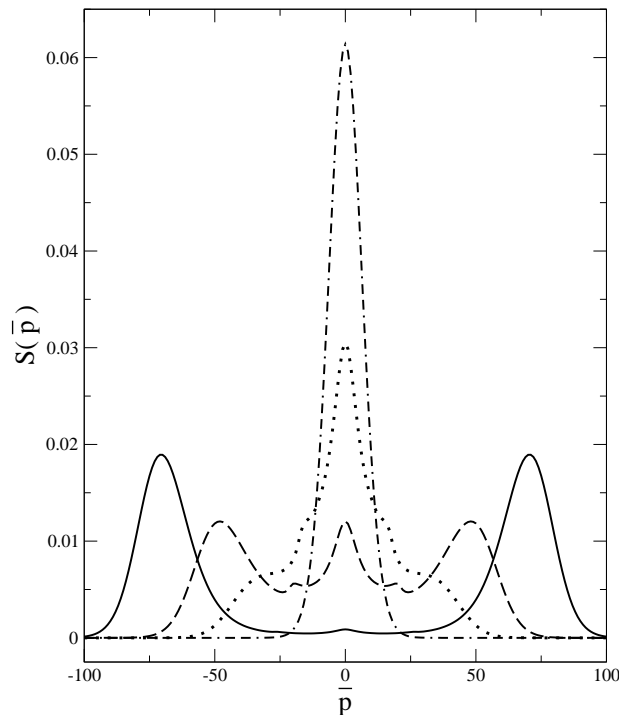


FIG. 7: Cuts in the momentum distribution of Fig.5 for $\tilde{\delta} = 0$ (dash-dotted line), 170(dotted line), 220(dashed line), 300(solid line).

V. SUMMARY

We have extended the calculations of I to allow for non-zero detuning in a standing-wave Raman scheme (SWRS) that results in reduced period optical lattices. The results differ from that of conventional Sisyphus cooling. Optimal cooling occurs for exact two-photon resonance, but many new and interesting features appear for non-zero detuning. A dressed atom picture was introduced, but had limited usefulness, owing to the presence of nonadiabatic transitions. In a future planned publication, we will look at Monte Carlo solutions to this problem and examine the dynamics of the velocity distribution. Specifically we will attempt to determine how the atomic momentum jumps between the momentum peaks shown in Fig. 5. Furthermore we will see if it is possible to localize atoms in the potential wells shown in Fig. 4. The ability to do so would imply separation of $\lambda/8$ between atoms in adjacent wells.

VI. ACKNOWLEDGMENTS

This research is supported by National Science Foundation under Grants No. PHY-0244841, PHY-0245522, and the FOCUS Center Grant. We thank G. Raithel and G. Nienhuis for helpful discussions.

Appendix

Using the Fourier series expansion

$$w(x) = \sum_n W_n e^{i2nx}, \quad (\text{A1})$$

in Eq. (16) we obtain the recursion relation

$$\begin{aligned} A_-(n)W_{n-1} + A_0(n)W_n + A_+(n)W_{n+1} = \\ S(p) [B_- \delta_{n,-1} + B_0 \delta_{n,0} + B_+ \delta_{n,1}] \\ + 2\hbar k \sigma \frac{\partial S}{\partial p} [B'_- \delta_{n,-1} + B'_0 \delta_{n,0} + B'_+ \delta_{n,1}], \end{aligned} \quad (\text{A2})$$

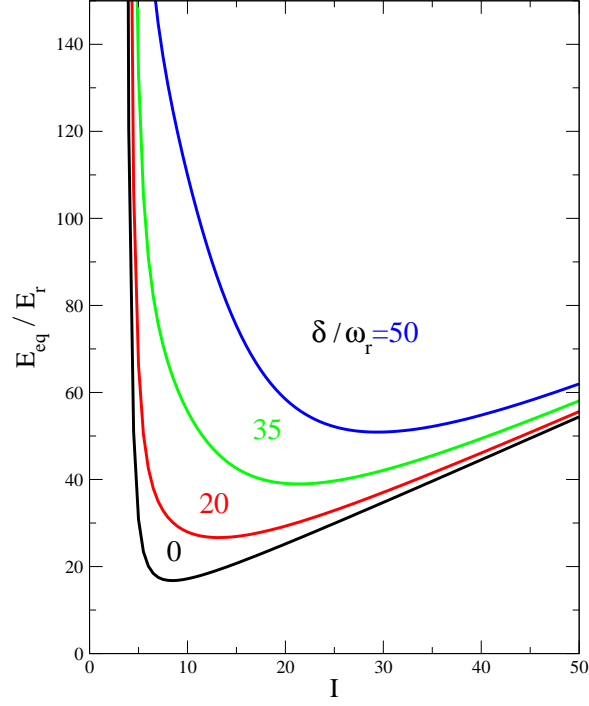


FIG. 8: Equilibrium energy in units of the recoil energy as a function of dimensionless intensity I for $\sigma = 10$ and $\tilde{\delta} = 0, 20, 35, 50$.

where

$$A_-(n) = \frac{\sigma^2}{1 + 2i\alpha} \frac{1 + i\alpha(2n - 1)}{d^2 + (1 + i\alpha(2n - 1))^2}, \quad (\text{A3a})$$

$$A_0(n) = 1 + \frac{\sigma^2}{1 + 2i\alpha} \left[\frac{1 + i\alpha(2n - 1)}{d^2 + (1 + i\alpha(2n - 1))^2} + \frac{1 + i\alpha(2n + 1)}{d^2 + (1 + i\alpha(2n + 1))^2} \right], \quad (\text{A3b})$$

$$A_+(n) = \frac{\sigma^2}{1 + 2i\alpha} \frac{1 + i\alpha(2n + 1)}{d^2 + (1 + i\alpha(2n + 1))^2}, \quad (\text{A3c})$$

$$B_- = \frac{\sigma}{2} \frac{1}{1 - i2\alpha} \frac{d}{d^2 + (1 - i\alpha)^2}, \quad (\text{A4a})$$

$$B_0 = \frac{\sigma}{2} \left\{ \frac{d}{d^2 + (1 - i\alpha)^2} + \frac{d}{d^2 + (1 + i\alpha)^2} \right\}, \quad (\text{A4b})$$

$$B_+ = \frac{\sigma}{2} \frac{1}{1 + i2\alpha} \frac{d}{d^2 + (1 + i\alpha)^2}, \quad (\text{A4c})$$

$$B'_- = \frac{i\sigma}{2} \frac{1}{1 - i2\alpha} \frac{d}{d^2 + (1 - i\alpha)^2}, \quad (\text{A5a})$$

$$B'_0 = \frac{i\sigma}{2} \left\{ \frac{d}{d^2 + (1 - i\alpha)^2} - \frac{d}{d^2 + (1 + i\alpha)^2} \right\}, \quad (\text{A5b})$$

$$B'_+ = -\frac{i\sigma}{2} \frac{1}{1 + i2\alpha} \frac{d}{d^2 + (1 + i\alpha)^2}. \quad (\text{A5c})$$

We are faced with solving the following equation:

$$\begin{pmatrix} \ddots & \ddots & 0 & 0 & 0 & 0 & 0 \\ \ddots & A_0(-2) & A_+(-2) & 0 & 0 & 0 & 0 \\ 0 & A_-(-1) & A_0(-1) & A_+(-1) & 0 & 0 & 0 \\ 0 & 0 & A_-(0) & A_0(0) & A_+(0) & 0 & 0 \\ 0 & 0 & 0 & A_-(1) & A_0(1) & A_+(1) & 0 \\ 0 & 0 & 0 & 0 & A_-(2) & A_0(2) & \ddots \\ 0 & 0 & 0 & 0 & 0 & \ddots & \ddots \end{pmatrix} \begin{pmatrix} \vdots \\ W_{-2} \\ W_{-1} \\ W_0 \\ W_1 \\ W_2 \\ \vdots \end{pmatrix} = \begin{pmatrix} \vdots \\ 0 \\ \tilde{B}_- \\ \tilde{B}_0 \\ \tilde{B}_+ \\ 0 \\ \vdots \end{pmatrix}, \quad (\text{A6})$$

where

$$\tilde{B}_j = S(p)B_j + 2\hbar k\sigma \frac{\partial S}{\partial p} B'_j, \quad (\text{A7})$$

and $j = \pm, 0$. From Eq. (A6), we see that for $n < -1$ and for $n > 1$

$$A_-(n)W_{n-1} + A_0(n)W_n + A_+(n)W_{n+1} = 0. \quad (\text{A8})$$

The final solution for the spatially averaged friction and diffusion coefficients depends only on $W_0, W_{\pm 1}$. However, to calculate these quantities all the other W s must be evaluated. In practice, we truncate Eq. (A6) by setting $W_{\pm n} = 0$ and then compare the solution with that obtained by setting $W_{\pm(n+1)} = 0$; when these solutions differ by less than a fraction of a percent, we use the result to evaluate $W_{\pm 2}/W_{\pm 1}$, from which one can then calculate $W_0, W_{\pm 1}$.

For $n > 1$, Eq. (A6) yields

$$W_n \left(1 + \frac{A_+(n) W_{n+1}}{A_0(n) W_n} \right) = -\frac{A_-(n)}{A_0(n)} W_{n-1},$$

which can be written in the form

$$\frac{W_n}{W_{n-1}} = -\frac{A_-(n)/A_0(n)}{1 + \frac{A_+(n) W_{n+1}}{A_0(n) W_n}}.$$

Setting $n = 2$ we obtain the continued fraction solution

$$C_+ = \frac{W_2}{W_1} = -\frac{A_-(2)/A_0(2)}{1 - \frac{A_+(2)}{A_0(2)} \frac{A_-(3)/A_0(3)}{1 - \frac{A_+(3)}{A_0(3)} \frac{A_-(4)/A_0(4)}{1 - \dots}}}. \quad (\text{A9})$$

Similarly, for $n < -1$ we find

$$C_- = \frac{W_{-2}}{W_{-1}} = -\frac{A_+(-2)/A_0(-2)}{1 - \frac{A_-(-2)}{A_0(-2)} \frac{A_+(-3)/A_0(-3)}{1 - \frac{A_-(-3)}{A_0(-3)} \frac{A_+(-4)/A_0(-4)}{1 - \dots}}}. \quad (\text{A10})$$

One can now use Eqs. (A6), (A9), (A10) to obtain equations for $W_0, W_{\pm 1}$ in terms of C_{\pm} and the \tilde{B}_j s. Explicitly, one finds

$$\begin{pmatrix} A_0(-1) + A_-(-1)C_- & A_+(-1) & 0 \\ A_-(0) & A_0(0) & A_+(0) \\ 0 & A_-(1) & A_0(1) + A_+(1)C_+ \end{pmatrix} \begin{pmatrix} W_{-1} \\ W_0 \\ W_1 \end{pmatrix} = \begin{pmatrix} \tilde{B}_- \\ \tilde{B}_0 \\ \tilde{B}_+ \end{pmatrix}. \quad (\text{A11})$$

The procedure is to obtain C_+ and C_- according to the continued fraction solutions Eq. (A9) and Eq. (A10) and then find $W_{-1,0,1}$ from Eq. (A11).

Next we calculate $\eta_{1,2}$, Eq.(18a)-(18b) using Eqs. (A1), (A11), (14a) as

$$\eta_1 = -\left[a_0 S + 2a_1 \hbar k \sigma \frac{\partial S}{\partial p} + W_0 a_2 + W_1 a_3 + W_{-1} a_4 \right] / 2, \quad (\text{A12a})$$

$$\eta_2 = -\left[b_0 S + 2b_1 \hbar k \sigma \frac{\partial S}{\partial p} + W_0 b_2 + W_1 b_3 + W_{-1} b_4 \right] / 2, \quad (\text{A12b})$$

where

$$a_0 = \int_0^\infty d\tau e^{-\tau} \cos(d\tau) \sin(\alpha\tau) = \frac{\alpha(1 - d^2 + \alpha^2)}{(1 + (d - \alpha)^2)(1 + (d + \alpha)^2)}, \quad (\text{A13a})$$

$$a_1 = \int_0^\infty d\tau e^{-\tau} \cos(d\tau) \cos(\alpha\tau) = \frac{(1 + d^2 + \alpha^2)}{(1 + (d - \alpha)^2)(1 + (d + \alpha)^2)}, \quad (\text{A13b})$$

$$a_2 = 2\sigma \int_0^\infty d\tau e^{-\tau} \sin(d\tau) \sin(\alpha\tau) = \frac{4\sigma d\alpha}{(1 + (d - \alpha)^2)(1 + (d + \alpha)^2)}, \quad (\text{A13c})$$

$$a_3 = i\sigma \int_0^\infty d\tau e^{-\tau} \cos(d\tau) e^{-i\alpha\tau} = \frac{i\sigma d}{d^2 + (1 + i\alpha)^2}, \quad (\text{A13d})$$

$$a_4 = -i\sigma \int_0^\infty d\tau e^{-\tau} \cos(d\tau) e^{i\alpha\tau} = \frac{-i\sigma d}{d^2 + (1 - i\alpha)^2}, \quad (\text{A13e})$$

$$b_0 = a_1, \quad (\text{A14a})$$

$$b_1 = -a_0, \quad (\text{A14b})$$

$$b_2 = 2\sigma \int_0^\infty d\tau e^{-\tau} \sin(d\tau) \cos(\alpha\tau) = \frac{2\sigma d(1 + d^2 - \alpha^2)}{(1 + (d - \alpha)^2)(1 + (d + \alpha)^2)}, \quad (\text{A14c})$$

$$b_3 = \sigma \int_0^\infty d\tau e^{-\tau} \cos(d\tau) e^{-i\alpha\tau} = \frac{\sigma d}{d^2 + (1 + i\alpha)^2}, \quad (\text{A14d})$$

$$b_4 = \sigma \int_0^\infty d\tau e^{-\tau} \cos(d\tau) e^{i\alpha\tau} = \frac{\sigma d}{d^2 + (1 - i\alpha)^2}. \quad (\text{A14e})$$

Since each W_i contains a term proportional to S and another term proportional to $\frac{\partial S}{\partial p}$, one has

$$W_i = \theta_i S + 2\hbar k \sigma \zeta_i \frac{\partial S}{\partial p}, \quad (\text{A15})$$

and Eqs.(A12) can be written as

$$\eta_1 = - \left[S(a_0 + \theta_0 a_2 + \theta_1 a_3 + \theta_{-1} a_4) + 2\hbar k \sigma \frac{\partial S}{\partial p} (a_1 + \zeta_0 a_2 + \zeta_1 a_3 + \zeta_{-1} a_4) \right] / 2, \quad (\text{A16a})$$

$$\eta_2 = - \left[S(b_0 + \theta_0 b_2 + \theta_1 b_3 + \theta_{-1} b_4) + 2\hbar k \sigma \frac{\partial S}{\partial p} (b_1 + \zeta_0 b_2 + \zeta_1 b_3 + \zeta_{-1} b_4) \right] / 2. \quad (\text{A16b})$$

Using Eqs. (A16) with the Fokker-Plank equations (17) and (19), one can identify the averaged force and diffusion coefficients appearing in Eqs. (20) with

$$\xi_f = (a_0 + \theta_0 a_2 + \theta_1 a_3 + \theta_{-1} a_4), \quad (\text{A17a})$$

$$\xi_{sp} = (b_0 + \theta_0 b_2 + \theta_1 b_3 + \theta_{-1} b_4), \quad (\text{A17b})$$

$$\xi_{st} = (a_1 + \zeta_0 a_2 + \zeta_1 a_3 + \zeta_{-1} a_4). \quad (\text{A17c})$$

- [1] P. R. Berman, G. Raithel, R. Zhang, and V. S. Malinovsky, Phys.Rev. A 72 (2005) 033415 . This article contains several additional references.
- [2] See, for example, A. Derevianko and C. C. Cannon, Phys. Rev. A 70 (2004) 062319.
- [3] This condition is necessary to neglect the effects of fields E_1 acting on the 2-3 transition and E_2 acting on the 1-3 transition with regards to light shifts and optical pumping; however, it is possible to neglect the effect of fields E_2 and E_1 driving coherent transitions between levels 1 and 2 (with E_2 acting on the 1-3 transition and E_1 acting on the 2-3 transition) under the much weaker condition that the optical pumping rates be much smaller than ω_{21} .
- [4] The condition needed to neglect modulated Stark shifts resulting from the combined action of fields E_1 and E_2 (or E_2 and E_4), as well as transitions between levels 1 and 2 resulting from fields E_1 and E_2 (or E_3 and E_2) is $|\Omega_3 - \Omega_1| \ll |\chi\chi'/\Delta|$ and $|\Omega_4 - \Omega_2| \ll |\chi\chi'/\Delta|$, where χ is a Rabi frequency associated with the 1-3 transition and χ' is a Rabi frequency associated with the 2-3 transition.

- [5] The interaction representation is one in which $\rho_{12}^{normal} = \rho_{12} e^{i(\Omega_1 - \Omega_2)t} = \rho_{12} e^{i(\Omega_3 - \Omega_4)t}$, where ρ_{12} is the density matrix element in the field interaction representation.
- [6] M Goldstein and R. M. Thaler, *Tables and Aids to Comp.* 12 (1958) 18; *ibid.* 13 (1959) 102.
- [7] J. Ziegler and P. R. Berman, *Phys.Rev. A* 16 (1977) 681.
- [8] J. Ziegler and P. R. Berman, *Phys.Rev. A* 15 (1977) 2042.
- [9] S-Q. Shang, B.Sheehy, P van der Straten, and H. Metcalf, *Phys. Rev. Lett.* 65 (1990) 317; P. Berman, *Phys. Rev. A* 43 (1991) 1470 [Note that Eq. (48) is valid only for $\Delta/\Gamma \lesssim 1$]; P. van der Straten, S-Q. Shang, B.Sheehy, H. Metcalf, and G. Nienhuis, *Phys. Rev. A* 47 (1993) 4160.
- [10] J. Dalibard and C. Cohen-Tannoudji, *J. Opt. Soc. B* 6 (1989) 2023.
- [11] As was discussed in I, in the limit that $\delta \sim 0$, it is more convenient to introduce "dressed" states via the definitions

$$\begin{aligned} |A\rangle' &= (|1\rangle + |2\rangle) / \sqrt{2}, \\ |B\rangle' &= (-|1\rangle + |2\rangle) / \sqrt{2}, \end{aligned}$$

with corresponding eigenvalues $\lambda_{\pm} = \pm 2\hbar\chi_{eff} \cos x$. These potentials cross, as shown in Fig. 7 (b) of I, but there is no coupling between the eigenstates. For $\delta \neq 0$, we have not found a general transformation that minimizes the nonadiabatic coupling.